Magnetic Properties

Building Molecular Minerals: All Ferric Pieces of Molecular Magnetite**

Guy W. Powell, Hannah N. Lancashire, Euan K. Brechin, David Collison,* Sarah L. Heath,* Talal Mallah, and Wolfgang Wernsdorfer*

Currently, there is a great deal of interest in the synthesis of transition-metal clusters that can behave as single-molecule magnets (SMMs).[1] An SMM requires effectively a combination of large spin ground state with a negative zero-field splitting (*D* value), which leads to magnetic bistability (hysteresis) that is the property of an individual molecule. These clusters may find potential uses in the information storage industry or as qubits in quantum computing.[2] One logical way to prepare SMMs is by synthesizing fragments of the naturally occurring magnetic oxides. This synthesis can be by either a top-down or bottom-up approach, that is, the breaking down or building up of a mineral lattice. Herein we report the synthesis of two iron oxy hydroxy clusters that represent two related portions of the magnetite lattice,

[*] G. W. Powell, H. N. Lancashire, Dr. E. K. Brechin,[+] Dr. D. Collison, Dr. S. L. Heath
Department of Chemistry
University of Manchester
Oxford Road, Manchester, M13 9PL (UK)
Fax: (+44) 161-275-4598
E-mail: euan.k.brechin@man.ac.uk
david.collison@man.ac.uk
sarah.l.heath@man.ac.uk

Prof. T. Mallah
Laboratoire de Chimie Inorganique
Université Paris Sud, UMR CNRS 8613, 91405 Orsay (France)

Dr. W. Wernsdorfer
Laboratoire Louis NeéL
CNRS, 25 Avenue des Martyrs BP166
38042 Grenoble Cedex 9 (France)

[+] Current address:
School of Chemistry
The University of Edinburgh
West Mains Road
Edinburgh, EH9 3JJ
E-mail: ebrechin@staffmail.ed.ac.uk

[**] This work was supported by The Royal Society of London, Lloyd's of London Tercentenary Foundation, The Nuffield Foundation, and the EPSRC (UK).

  DOI: 10.1002/ange.200460636

constructed by a bottom-up approach and utilizing ligand-controlled hydrolysis of a metal salt to determine the extent of cluster aggregation.

$[Fe_9O_4(OH)_5(heia)_6(Hheia)_2]\cdot 3.5\,CH_3OH\cdot 8\,H_2O$ (**1**; $H_2heia = HN\{CH_2COOH\}CH_2CH_2OH$; Figure 1) was synthesized by reaction of iron(III) nitrate nonahydrate with H_2heia and tetramethylammonium hydroxide in methanol. The hydrolysis was gradually stopped by evaporating the reaction mixture to dryness. Crystals of **1** suitable for single crystal X-ray diffraction were obtained after 2 weeks by crystallization from a MeOH solution of **1** in the presence of liquid drying agent (diethoxymethane) to hinder further hydrolysis.[3] $Hpy[Fe_{17}O_{16}(OH)_{12}(py)_{12}Cl_4]Cl_4\cdot 4.5\,CH_3OH$ (**2**; py = pyridine; Figure 2) was prepared by the reaction of anhydrous iron(III) chloride in pyridine in a flask open to the atmosphere at room temperature, and crystals of **2** suitable for single crystal X-ray diffraction were isolated in low yield after diffusion of methanol over 2 weeks.[3]

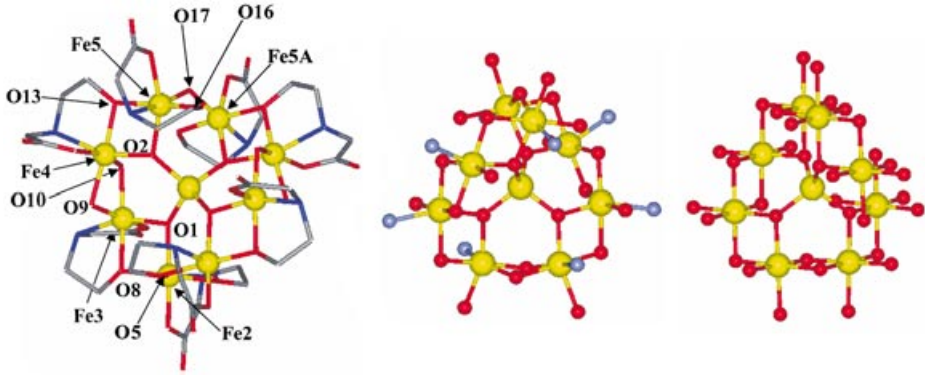

Figure 1. The molecular structure of the cluster in **1** (left), the core of **1** (middle), and its relation to magnetite (right); yellow Fe, red O, blue N, gray C.

The complex in **1** is constructed from a central tetrahedral Fe^{III} ion which links, by four μ_3-oxo bridges, to the outer eight iron atoms. Each of the outer iron ions is capped by a facially coordinated heia ligand and has distorted octahedral coordination geometry. Six of the heia ligands are fully deprotonated and the alcohol arm of these ligands (O5, O8, O13 and their symmetry equivalents) bridges between pairs of outer irons: the second bridge between these irons is from the inner μ_3-oxo ligands. The remaining two Hheia ligands have protonated alcohol arms (O16 and its symmetry equivalent) that coordinate terminally. Two of the outer irons (Fe3 and Fe4) are bridged by two μ_2-hydroxo ligands (O9 and O10) and two others, Fe5 and Fe5A, are bridged by a single hydroxo ligand (O17). This asymmetry in the mode (and hence angle) of the bridging between the outer iron ions has consequences for the magnetic exchange pathways in **1** (see below). The bromide analogue of **2** can be prepared by a similar route in higher yield and has a cluster that is isostructural with the chloride; this will be reported in detail elsewhere.

The complex in **2** also has at its core a central tetrahedral Fe^{III} ion, but in contrast to **1** this is linked by μ_4-oxo bridges to twelve outer octahedral Fe^{III} ions, which form a truncated tetrahedron: the octagonal faces of this tetrahedron (Fe2, Fe3, Fe5, Fe7, and symmetry equivalents) are capped by four further iron ions (Fe4, Fe6, and symmetry equivalents), linked by a combination of μ_3-oxo and μ_2-hydroxo ligands. The inner Fe^{III} ion and the four outer Fe^{III} ions of **2** sit in the tetrahedral sites of the lattice with the others occupying the octahedral sites. The chloride ions cap the outer tetrahedrally coordinated Fe^{III} ions with the pyridine molecules capping the octahedrally coordinated Fe^{III} ions.

A closer inspection of the cores of **1** and **2** reveals that both are fragments of the iron and oxygen positions defined by the magnetite lattice as shown in the comparison of **1** and **2** to their corresponding fragments of magnetite in Figures 1 and 2. Compound **1** is formally converted into **2** by adding a layer of Fe ions through the conversion of μ_3-oxo into μ_4-oxo

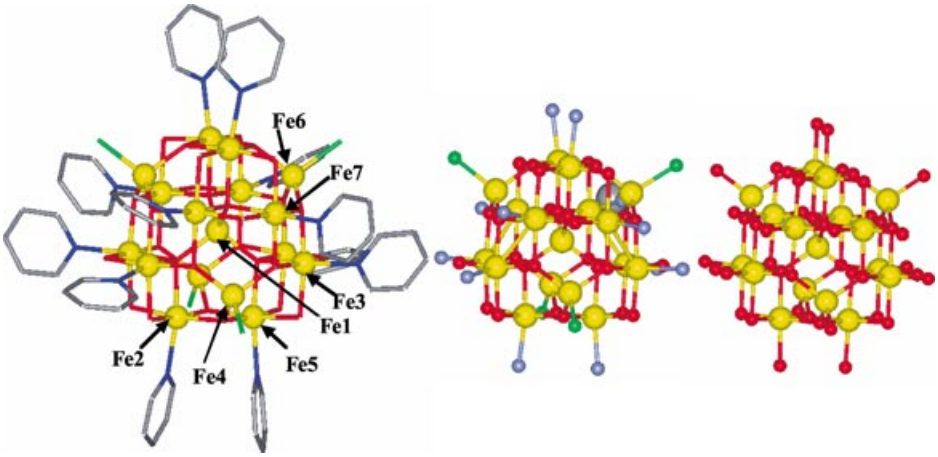

Figure 2. The molecular structure of the cluster in **2** (left), the core of **2** (middle), and its relation to magnetite (right); yellow Fe, red O, blue N, gray C, green Cl).

ligands. Many of the polynuclear transition-metal clusters isolated to date, that resemble mineral units, are fragments of the $M(OH)_2$ brucite lattice.[4] In our case, **1** is formed by restricting the hydrolysis from a hydrated iron(III) salt using a facially capping tridentate ligand with "arms" of very different pK_a values. In contrast, **2** is produced by restricting the amount of hydrolytic source in a basic, strongly coordinating medium. The isolation of **2**, in particular, suggests that larger fragments of "molecular magnetite" can be isolated by using coordinating bases of differing strengths.

In both **1** and **2** all the iron centers (both tetrahedral and octahedral) are Fe^{III} ions, this is confirmed by charge-balance considerations and bond valence sum (BVS) calculations.[5] This result is in contrast to the situation in magnetite where half the octahedral sites in the lattice are occupied by Fe^{II} ions. The assignment of hydroxo versus oxo was achieved on the basis of geometry and BVS calculations.

The magnetic properties of **1** and **2** were examined using variable-temperature magnetic measurements on bulk powdered samples (300–1.8 K, 0.1–5.5 T) and on single crystals to mK temperatures on a micro-SQUID. Susceptibility data for both **1** and **2** indicate the presence of antiferromagnetic interactions, with low-temperature maxima suggesting large spin ground states. To determine the value of the spin ground state for **1** and **2**, magnetization measurements were performed at 2–6 K between 0.1 and 5.5 T. For **1** the best fit (first made for each temperature independently and second by simultaneously fitting the data for the three temperatures for an isolated ground state) was obtained for $S = 25/2$, $g = 1.99$, and $D = -0.07\ cm^{-1}$ (Figure 3). For **2** the initial best fit was for $S = 35/2$ as the ground state with the following parameters: $g = 1.96$ and $D = +0.33\ cm^{-1}$ (Figure 4), see below. The occurrence of such large spin ground states for both complexes arises from the presence of competing antiferromagnetic and ferromagnetic exchange-coupling interactions between the octahedral and tetrahedral Fe^{III} ions. Closer

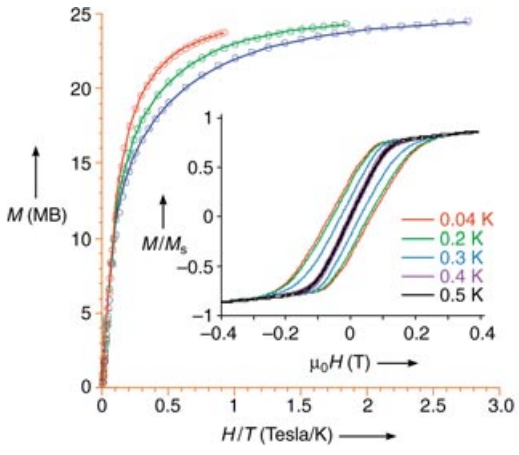

Figure 3. Plot of magnetization (M) versus H/T for **1** in the ranges 0.1–5.5 T and 2 (○), 3 (○), and 6 K (○). The solid lines are fits to $S = 25/2$, $g = 1.99$, $D = -0.07\ cm^{-1}$. Inset: magnetization of **1** plotted as a fraction of the saturation value M_s versus applied magnetic field ($\mu_0 H$) at sweep rates of 0.007 $T s^{-1}$ and T = 0.1–0.5 K. S = Spin quantum number of the cluster, g = g value of cluster, D = axial zero-field splitting parameter.

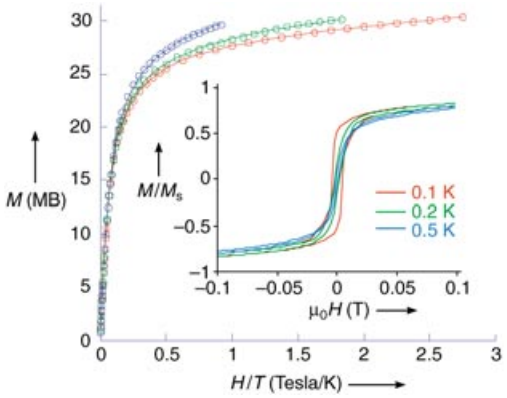

Figure 4. Plot of magnetization (M) versus H/T for **2** in the ranges 0.1–5.5 T and 2 (○), 3 (○), and 6 K (○). The solid lines are fits to $S = 35/2$, $g = 1.96$, $D = +0.33\ cm^{-1}$. Inset: magnetization of **2** plotted as a fraction of the saturation value M_s versus applied magnetic field ($\mu_0 H$) at sweep rates of 0.001 $T s^{-1}$ and T = 0.04–0.5 K.

examination of the structure of **1** reveals that the Fe-O-Fe bridges fall into two clear categories: those that connect the central tetrahedral Fe^{III} centers to the outer octahedral Fe^{III} centers (by the oxo ligands) are all characterized by angles in the range 125–130°, and those that bridge between the Fe^{III} ions in the outer octametallic "twisted ribbon" are characterized by angles in the range 97–101°. If we assume that the largest Fe-O-Fe angles promote the strongest antiferromagnetic interaction then we are left with a situation where the central tetrahedral Fe^{III} center is antiferromagnetically coupled to all the octahedrally coordinated Fe^{III} ions, which leads to an $S = 35/2$ spin ground state. However, there is one anomaly in the bridging angles connecting the outer octahedrally coordinated Fe ions: the angle between Fe5 and Fe5A through O17 is 130°. This angle is bigger than the angle connecting either Fe5 or Fe5A to the central metal ion and so we might consider the exchange between the Fe5/Fe5A pair to be dominant, and antiferromagnetic. This situation would lead to a molecule with two "spin up" and seven "spin down" $S = 5/2$ centers and an overall spin ground state of $S = 25/2$, consistent with that obtained from the magnetization measurements.

For complex **2**, the same argument applies: the antiferromagnetic interactions between the tetrahedrally and octahedrally coordinate Fe^{III} ions (through Fe-O-Fe angles of 122–126° compared to 94–98° between the octahedral Fe centers) dominate, which leads to a situation in which the five tetrahedrally coordinated Fe^{III} ions are "spin up" and the twelve octahedrally coordinated Fe^{III} ions are "spin down" giving an overall $S = 35/2$ ground state.

To examine the low-temperature magnetic behavior of **1** and **2**, single crystal magnetization measurements were performed on them using an array of micro-SQUIDS.[6] Relaxation data for **1** were determined from direct current (dc) relaxation-decay measurements: a large dc field of 1.4 T was applied to the sample at 5 K to saturate the magnetization in one direction, and the temperature lowered to a specific value between 1.0 and 0.04 K. When the temperature was stable the field was swept from 1.4 T to zero at a rate of

$0.14\ T\,s^{-1}$ and the magnetization in zero-field measured as a function of time. This method allows the construction of an Arrhenius plot of $\ln\tau$ versus $1/T$, which shows that above approximately 0.15 K the relaxation rate is temperature dependent. The fit to an Arrhenius law yields $\tau_0 = 6\times10^{-10}$ s and $U_{eff} = 7.6$ K. However, below approximately 0.15 K the relaxation rate is temperature independent with a value of 8×10^3 s, indicative of quantum tunneling of the magnetization (QTM) between the lowest energy $M_s = \pm 25/2$ levels of the ground state. Hysteresis loops for **1** (inset, Figure 3) are observed at temperatures below 0.5 K and at sweep rates of $0.001\ T\,s^{-1}$, with the field applied in the direction of the easy-axis of the molecules. The hysteresis loops do not show steps at regular intervals of field, indicative of resonant QTM, but are smooth. The steps may be present, but simply broadened out by intermolecular antiferromagnetic interactions between the separate Fe_9 molecules. Indeed, a Curie–Weiss plot suggests antiferromagnetic intermolecular interactions in the order of approximately −0.7 K. Further geometric analysis of **1** shows that the metallic cluster approximates to an oblate spheroid of estimated core dimensions 6.38 × 6.25 Å, and the nearest neighbor intercentroid separations in the lattice are 12.13 and 15.49 Å.

Low-temperature single-crystal magnetic measurements on **2** (inset, Figure 4) using the methods described in the investigation of **1**, show no signs of SMM behavior. The small hysteresis loops observed below approximately 0.5 K result from long-range ferromagnetic ordering between the individual Fe_{17} molecules and not from the presence of molecular anisotropy. The anomalously large zero-field splitting and low g value (for Fe^{III}, typical parameters are $g \approx 2.00$ and $|D| \leq 0.2\ cm^{-1}$) obtained for **2** using a model for magnetization in an isolated spin state (see above) might also suggest the presence of long-range interactions. We would expect the cluster g and D values to be similar to those of the isolated Fe^{III} centers in this case. In **2** the core of the cluster is much more spherical than that in **1** (although it has 12 protruding pyridine rings) with a diameter of the metallic core of approximately 6.96 Å and nearest neighbor intercentroid separations of 14.89 and 16.12 Å. The pyridine rings show no obvious π-stacking interactions between clusters.

For both **1** and **2** the magnetic behavior is comparable to that observed in magnetite, wherein the iron ions in the octahedral and tetrahedral holes are antiferromagnetically coupled, but net magnetization results from the noncompensated spin of the Fe^{II} ions which occupy one quarter of the octahedral sites.

In conclusion, it is possible to construct high-spin molecules, single-molecule magnets, and molecular mineral analogues using a simple bottom-up, controlled hydrolysis approach. That the iron ions in **1** and **2** are all ferric and hence almost electronically isotropic (i.e. $|D|$ is small), probably prevents more exciting magnetic behavior. However, since these clusters form part of a naturally occurring mixed-valence mineral, the reduction of some Fe^{III} ions to form complexes more reminiscent of the parent mineral, remains a possibility, as does incorporation of Fe^{II} during synthesis. Thus, inclusion of some of the much more anisotropic Fe^{II} ions into this new structural family might be expected to increase substantially the overall zero-field splitting of the clusters.

Experimental Section

1: A solution of heiaH_2 (0.595 g, 5.0 mmol) and $N(CH_3)_4(OH)\cdot5H_2O$ (2.265 g,12.5 mmol) in MeOH (10 mL) was added slowly to a stirred solution of $Fe(NO_3)_3\cdot9H_2O$ (1.01 g, 2.5 mmol) in MeOH (10 mL). The reaction mixture was allowed to evaporate to dryness over a period of 2 days, before extracting into diethoxymethane (3.1 mL, 25 mmol) and MeOH (6.9 mL). Solids ($N(CH_3)_4(NO_3)$) were removed by filtration and acetone diffused slowly into the filtrate to yield crystals suitable for single-crystal X-ray diffraction after 2 weeks. Elemental analysis calcd (%) for $Fe_9C_{35.5}H_{93}O_{44.5}N_8$: C 23.09, H 5.08, N 6.07, Fe 27.22; found: C 23.65, H 5.35, N 6.38, Fe 27.48.

2: $FeCl_3$ (0.910 g, 3.09 mmol) was added to stirred pyridine (30 mL), the reaction mixture became dark upon dissolution. After stirring for 2 h the reaction mixture was filtered, the filtrate was collected and methanol diffused in slowly to afford single crystals suitable for X-ray diffraction after two weeks. Elemental analysis calcd (%) for $Fe_{17}C_{69.5}H_{102}O_{35.5}N_{13}Cl_8$: C 28.71, H 2.62, N 6.70, Fe 35.03; found: C 28.62, H 2.59, N 6.75, Fe 35.84.

Received: May 12, 2004

Keywords: cluster compounds · hydrolysis · iron · magnetic properties · single-molecule magnets

[1] a) D. Gatteschi, R. Sessoli, *Angew. Chem.* **2003**, *115*, 278; *Angew. Chem. Int. Ed.* **2003**, *42*, 268; b) R. Sessoli, D. Gatteschi, D. N. Hendrickson, G. Christou, *MRS Bull.* **2000**, *25*, 66; c) W. Wernsdorfer, R. Sessoli, *Science* **1999**, *284*, 133; d) S. Hill, R. S. Edwards, N. Aliaga-Alcalde, G. Christou, *Science* **2003**, *302*, 1015; e) A. J. Tasiopoulos, A. Vinslava, W. Wernsdorfer, K. A. Abboud, G. Christou, *Angew. Chem.* **2004**, *116*, 2169; *Angew. Chem. Int. Ed.* **2004**, *43*, 2117.

[2] M. N. Leuenberger, D. Loss, *Nature* **2001**, *414*, 789.

[3] Crystallographic details for **1**: $Fe_9C_{35.5}H_{93}O_{44.5}N_8$, $M_r = 1846.83$, crystal size $0.05\times0.02\times0.01\ mm^3$, trigonal, space group, $P3(2)21$, $a = b = 21.014(10)$, $c = 16.690(11)$ Å, $V = 6383(6)$ Å^3, $T = 100(2)$ K, $Z = 3$, $\rho_{calcd} = 1.441\ g\,cm^{-3}$, $\mu(\lambda = 0.71073\ Å) = 1.574\ mm^{-1}$, 28834 reflections collected, 6224 unique ($R_{int} = 0.1154$), $R(F) = 0.0602$ and $wR2 = 0.1678$ using 5936 reflections with $I > 2\sigma(I)$. **2**: $Fe_{17}C_{69.5}H_{102}O_{35.5}N_{13}Cl_8$, $M_r = 2920.69$, crystal size $0.50\times0.50\times0.20\ mm^3$, trigonal, space group, $R\bar{3}$, $a = b = 16.1170(9)$, $c = 69.928(6)$ Å, $V = 15730.9(19)$ Å^3, $T = 100(2)$ K, $Z = 6$, $\rho_{calcd} = 1.850\ g\,cm^{-3}$, $\mu(\lambda = 0.71073\ Å) = 2.556\ mm^{-1}$, 23613 reflections collected, 5023 unique ($R_{int} = 0.1424$), $R(F) = 0.0529$ and $wR2 = 0.1428$ using 4469 reflections with $I > 2\sigma(I)$. CCDC-238304 (**1**) CCDC-238305 (**2**) contains the supplementary crystallographic data for this paper. These data can be obtained free of charge via www.ccdc.cam.ac.uk/conts/retrieving.html (or from the Cambridge Crystallographic Data Centre, 12 Union Road, Cambridge CB2 1EZ, UK; fax: (+44) 1223-336-033; or deposit@ccdc.cam.ac.uk).

[4] see for examples a) J. C. Goodwin, R. Sessoli, D. Gatteschi, W. Wernsdorfer, A. K. Powell, S. L. Heath, *J. Chem. Soc. Dalton Trans.* **2000**, 1835; b) R. E. P. Winpenny, *J. Chem. Soc. Dalton Trans.* **2002**, 1; and a recent extension of this observation in J. C. Goodwin, S. J. Teat, S. L. Heath, *Angew. Chem.* **2004**, *116*, 4129; *Angew. Chem. Int. Ed.* **2004**, *43*, 4037.

[5] a) W. Liu, H. Thorp, *Inorg. Chem.* **1993**, *32*, 4102; b) I. D. Brown, D. Altermatt, *Acta Crystallogr. Sect. B* **1985**, *41*, 244.

[6] W. Wernsdorfer, *Adv. Chem. Phys.* **2001**, *118*, 99.

